Journal of the Egyptian Mathematical Society 25 (2017) 375–381

Contents lists available at ScienceDirect

Journal of the Egyptian Mathematical Society

journal homepage: www.elsevier.com/locate/joems

Original Article

Homotopy perturbation method for MHD pulsatile non-Newtonian nanofluid flow with heat transfer through a non-Darcy porous medium

N.T. Eldabe, M.Y. Abou-zeid*

Department of Mathematics, Faculty of Education, Ain Shams University, Heliopolis, Cairo, Egypt

ARTICLE INFO

Article history:
Received 20 October 2016
Revised 25 February 2017
Accepted 18 May 2017
Available online 12 June 2017

Keywords:
Pulsatile flow
Non-Newtonian nanofluid
Non-Darcy porous medium
Heat transfer
76: Fluid mechanics
34: Ordinary differential equations
80: Classical thermodynamics
Heat transfer

ABSTRACT

In this contribution, the MHD pulsatile mechanism with heat transfer of an incompressible non-Newtonian nanofluid between two permeable parallel vertical plates is investigated. The effects of non-Darcy porous medium, radiation, Ohmic and viscous dissipation are included. By using the homotopy perturbation method, a solution is obtained, which is in a good agreement with the momentum, energy and nanoparticles equations. Numerical results for the velocity, temperature and nanoparticles distributions are obtained.

1. Introduction

Nanofluids means the addition of nanoparticles to conventional working fluids that is containing a liquid of nanometer-sized particles which can improve heat transfer and solar energy collection. Recently, nanofluids attracts a great deal of interest with their enormous potential to provide enhanced performance properties, particularly with respect to heat transfer. Nanoparticles in the base fluid (nanofluid) provide the following possible advantages in the solar energy absorption system: (i) nanofluids can absorb energy with a directly- skipping intermediate heat transfer step, (ii) nanofluids can be optically selective (i.e., high absorption in the solar range and low emittance in the infrared), (iii) a more uniform receiver temperature can be achieved inside the collector (reducing material constraints), (iv) enhanced heat transfer via greater convection and thermal conductivity may improve the performance of the receiver, and (v) absorption efficiency may be enhanced by tuning the nanoparticle size and shape regarding to the proposed application [1].

Due to the bright future which is predicted for nanofluids, several studies of convective heat transfer in nanofluids have been conducted, recently. Hayat et al. [2] studied flow with heat transfer of nanofluid with mixed convection and non-linear thermal radiation effects in an inclined stretching sheet. Stagnation point flow of nanofluid with melting heat transfer is analyzed by Hayat et al. [3]. They considered heat generation/absorption effect as well as new condition of mass flux. Akdag et al. [4] studied numerically the heat transfer characteristics of Al2O3–water based nanofluids in a wavy mini-channel under pulsating inlet flow conditions. Hayat et al. [5] investigated the problem of MHD Falkner–Skan flow of a second grade nanofluid in a stretching wedge with melting heat transfer and heat generation/absorption effects. Maxwell nanofluid steady flow with heat transfer is studied by Hayat et al. [6] in the presesnce of applied magnetic field and thermal radiation effects. Selimefendigil and Öztop [7] discussed the application of the system identification method for forecasting the thermal performance of forced pulsating flow at a backward facing step with a stationary cylinder subjected to nanofluid. Hayat et al. [8] used HAM to solve the problem of porous medium MHD stretched flow of nanofluid. (MHD) flow of non-Newtonian nanofluid over a non-linear stretching sheet with heat and mass transfer are addresses by Hayat et al. [9]. They constructed new condition having zero mass flux of nanoparticles at the boundary. Pulsating flow and heat transfer of nanofluid in horizontal tube for the first time is studied numerically by Rahgoshay et al. [10].

* Corresponding author.
E-mail address: master_math2003@yahoo.com (M.Y. Abou-zeid).

http://dx.doi.org/10.1016/j.joems.2017.05.003

Nomenclature

A	The dimensional chemical reaction parameter
b	Forschheimer's constant
B_n	Bingham number $(\tau_y h/\mu V_0)$
Br	The local nanoparticle Grashof number $(\nu g\beta_f (f_o - f_1)/{V_0}^3)$
c_p	Specific heat at constant pressure
Da	Darcy number (k_p/h^2)
DB	Brownian diffusion coefficient
DT	The thermophoretic diffusion coefficient
e_{ij}	the (i,j) component of the deformation rate
Ec	Eckert number $({V_0}^2/c_p (T_0 - T_1))$
f	The nanoparticle phenomena
f_o, f_1	The nanoparticle at the walls
Fs	Forschheimer number $(h\,b)$
Gr	Grashof number $(\nu g\beta_T (T_o - T_1)/{V_0}^3)$
g	Acceleration due to gravity
k_T	The effective thermal conductivity
M	Magnetic field parameter $(\sigma B_0^2 h/\rho V_0)$
N_b	Brownian motion parameter
N_t	The thermophoresis parameter
Pr	Prandtl number (ν/k_T)
Q_0	Heat absorption coefficient
$\overline{Q}_1$	Absorption of radiation parameter
Q1	Heat absorption parameter $(Q_0 \nu/\rho c_p {V_0}^2)$
Q2	Dimensionless absorption of radiation parameter $(\overline{Q}_1 \nu (f_o - f_1)/{V_0}^2 (T_0 - T_1))$
q	Homotopy perturbation parameter
Sc	Schmidt number (ν/D_B)
T	The temperature
T_o, T_1	The temperature at the walls
t	The time
u, v	Component of velocity along x; y directions
V_0	Suction velocity
x, y	Distances along and perpendicular to the walls

Greek symbols

β_f	Nanoparticle expansion coefficient
β_T	The thermal expansion coefficient
δ	The dimensionless chemical reaction parameter
μ	The dynamic viscosity
ν	The kinematic viscosity
ω	Frequency of oscillations
ρ	The density
σ	The fluid electrical conductivity
τ_{ij}	The stress tensor
τ_y	The yield stress

There has been an interest in Darcy and non-Darcy flow in Newtonian and non-Newtonian fluid flow saturating porous medium. This continuing interest due to its applications such as chemical reactors, building insulation, packed bed, enhanced oil recovery, food technology and filtration processes. A square velocity term is added to Darcian velocity in momentum equation by Forchheimer [11]. Shehzad et al. [12] discussed the properties of Darcy-Forchheimer flow of an Oldroyd-B liquid. They considered Cattaneo-Christov heat flux theory in energy equation. The Darcy-Forchheimer flow of Maxwell fluid in the presence of temperature-dependent thermal conductivity is studied by Hayat et al. [13].

The study of the influence of pulsatile flow with heat transfer of Newtonian and non-Newtonian fluids in circular tubes has become important during recent years. This importance is due to their immediate practical applications in the lubrication technology, biophysical flows and many other day-to-day problems of transporation of different types of fluids. The analysis of the mechanisms responsible for pulsatile transport have been studied by many authors. Eldabe et al. [14,15] studied pulsatile MHD viscoelastic flow through a channel bounded by two permeable parallel plates and the effect of couple stresses on pulsatile hydromagnetic poiseuille flow. The theoretical and experimental studies of the blood flow phenomena are very useful for clinical purposes. Hayat et al. [16] analyzed the peristaltic flow of pseudoplastic fluid under the radially imposed magnetic field and convective heat and mass conditions. In some pathological situations, the distribution of fatty cholesterol and artery clogging blood clots in the lumen of the coronary artery can be considered as equivalent to a fictitious porous medium. Chaturani and Nandal [17] presented the mathematical model for pulsatile blood flow in a distencible aotie bifurcation subject to body acceleration. The effect of the chemical reaction and radiation absorption on the unsteady free convective flow of an incompressible viscous fluid through porous medium past a semi-infinite vertical permeable moving plate is studied by Eldabe et al. [18].

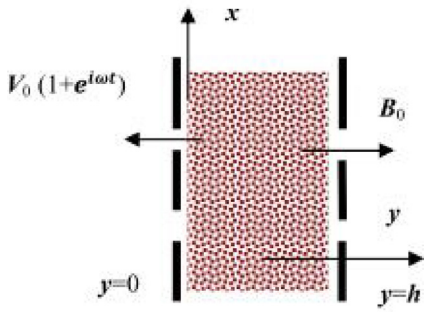

Fig. 1. Geometry of the problem.

In the present study, we extend the work of Eldabe et al. [18] with different surface to obtain analytical solution. The problem of MHD pulsatile flow of a Bingham non-Newtonian nanofluid with heat transfer through a non-Darcy porous medium between two permeable parallel vertical plates is studied. Effects of free convection, Ohmic and viscous dissipation, chemical reaction and radiation absorption is taken into our consideration. Solutions for the velocity, energy and nanoparticles equations are obtained by using Homotopy perturbation method (HPM). Numerical results for the velocity, temperature and nanoparticles phenomena distributions are obtained.

2. Mathematical models

We consider the unsteady flow with heat transfer of a viscous, incompressible, and electrically conducting non-Newtonian nanofluid (Bingham fluid) in a non-Darcy porous medium between two permeable parallel vertical plates situated at $y = 0$ and h. This kind of flow has received almost no attention despite applications such as flow in geological fractures and liquid cooling of finned heat exchanger tubes. The coordinates system used is given in Fig. 1. x and y axes are assigned to the direction of the flow and normal to the plates. We take into account free convection, chemical reaction, radiation absorption, viscous and Ohmic dissipations. Also, the flow is stressed by a uniform magnetic field B_0 acting along y- axis.

Since the two walls are infinite in a finite range, then all quantities are functions of y and t only, The fluid is being sucked outside the wall $y = 0$ and $y = h$ with uniform velocity $v = -V_0\,(1 + e^{i\omega t})$.

By employing the Bingham model [19] to describe the non-Newtonian fluid, as:

$$\tau_{ij} = \begin{cases} \tau_y + e_{ij}, & |\tau_{ij}| > |\tau_y|, \\ \tau_y, & |\tau_{ij}| \le |\tau_y|. \end{cases} \quad (1)$$

The basic non-dimensional equations governing MHD convective non-Newtonian nanofluid flow with heat transfer are as [17,18]:

$$\frac{\partial u}{\partial t} - (1 + e^{i\omega t})\frac{\partial u}{\partial y} = \left(B_n + \frac{\partial^2 u}{\partial y^2}\right) - \left(M + \frac{1}{Da}\right)u - Fs\,u^2 + Gr\,T + Br\,f, \quad (2)$$

$$\frac{\partial T}{\partial t} - (1 + e^{i\omega t})\frac{\partial T}{\partial y} = \frac{1}{\Pr}\frac{\partial^2 T}{\partial y^2} + Ec\left(B_n + \frac{\partial u}{\partial y}\right)\left(\frac{\partial u}{\partial y}\right) + Ec\left(M + \frac{1}{Da}\right)u^2 - Q_1\,T + Q_2\,f + N_b\left(\frac{\partial T}{\partial y}\frac{\partial f}{\partial y}\right) + N_t\left(\frac{\partial T}{\partial y}\right)^2, \quad (3)$$

$$\frac{\partial f}{\partial t} - (1 + e^{i\omega t})\frac{\partial f}{\partial y} = \frac{1}{Sc}\frac{\partial^2 f}{\partial y^2} + \frac{N_t}{N_b}\left(\frac{\partial^2 T}{\partial y^2}\right) - \delta\,f, \quad (4)$$

with the appropriate boundary conditions

$$\left.\begin{array}{llllll} u = 0, & T = 1 & \text{and} & f = 1 & \text{at} & y = 0 \\ u = 0, & T = 0 & \text{and} & f = 0 & \text{at} & y = 1 \end{array}\right\}, \quad (5)$$

where the dimensionless parameters were defined in nomenclature.

We also note that if $Ec = B_n = N_t = N_b = 0$, Eqs. (2)-(4) will reduce to that of Eldabe et al. [18]. Also, B_n is only vanished for ordinary Newtonian nanofluid. Pulsatile flow is a linear combination of the steady part and the oscillatory part. Based on this consideration, we present the solution for any function in the general form as follows:

$$g(y,\,t) = g_s(y) + g_0(y)\,e^{i\omega t}, \quad (6)$$

where g may be represent any of the physical quantities such as u, T, and f. g_s and g_0 are the steady and the oscillatory parts, respectively.

3. HPM method

We apply the homotopy perturbation method (HPM) [20–23] to the system of non-linear differential Eqs. (2)-(4) subject to boundary conditions (5). First, by employing HPM method

$$H(p,\,u_s) = (1-q)\left(L(u_s) - L(u_s^0)\right) + q\left(L(u_s) + B_n + \frac{du_s}{dy} - \left(M + \frac{1}{Da}\right)u_s - Fs\,u_s^2 + Gr\,T_s + Br\,f_s\right), \quad (7)$$

$$H(p,\,u_0) = (1-q)\left(L(u_0) - L(u_0^0)\right) + q\left(L(u_0) + \frac{du_s}{dy} + \frac{du_0}{dy} - \left(M + \frac{1}{Da} + i\omega\,u_0\right)u_0 - 2\,Fs\,u_s\,u_0 + Gr\,T_0 + Br\,f_0\right), \quad (8)$$

$$H(p,\,T_s) = (1-q)\left(L(T_s) - L(T_s^0)\right) + q\left(L(T_s) + \Pr\left(\frac{dT_s}{dy} + Ec\left(B_n + \frac{du_s}{dy}\right)\left(\frac{du_s}{dy}\right) + Ec\left(M + \frac{1}{Da}\right)u_s^2 - Q_1\,T_s + Q_2\,f_s + N_b\left(\frac{dT_s}{dy}\frac{df_s}{dy}\right) + N_t\left(\frac{dT_s}{dy}\right)^2\right)\right), \quad (9)$$

$$H(p,\,T_0) = (1-q)\left(L(T_0) - L(T_0^0)\right) + q\left(L(T_0) + \Pr\left(\frac{dT_s}{dy} + \frac{dT_0}{dy} + Ec\left(B_n + 2\frac{du_s}{dy}\right)\left(\frac{du_0}{dy}\right) + 2\,Ec\left(M + \frac{1}{Da}\right)u_s\,u_0 - (Q_1 + i\omega)T_0 + Q_2\,f_0 + N_b\left(\frac{dT_s}{dy}\frac{df_0}{dy} + \frac{dT_0}{dy}\frac{df_s}{dy}\right) + 2N_t\left(\frac{dT_s}{dy}\right)\left(\frac{dT_0}{dy}\right)\right)\right), \quad (10)$$

$$H(p,\,f_s) = (1-q)\left(L(f_s) - L(f_s^0)\right) + q\left(L(f_s) + Sc\left(\frac{df_s}{dy} + \frac{N_t}{N_b}\left(\frac{d^2T_s}{dy^2}\right) - \delta\,f_s\right)\right), \quad (11)$$

$$H(p,\,f_0) = (1-q)\left(L(f_0) - L(f_0^0)\right) + q\left(L(f_0) + Sc\left(-i\omega\,f_0 + \frac{df_s}{dy} + \frac{df_0}{dy} + \frac{N_t}{N_b}\left(\frac{d^2T_0}{dy^2}\right) - \delta\,f_0\right)\right), \quad (12)$$

with $L = \frac{d^2}{dy^2}$ as the linear operator, the initial approximations u_s^0, u_0^0, T_s^0, T_0^0, f_s^0 and f_0^0 can be defined as

$$\left.\begin{array}{l} u_s^0 = u_0^0 = T_0^0 = f_0^0 = y^2 - y \\ T_s^0 = f_s^0 = 1 - y \end{array}\right\}. \quad (13)$$

And assuming that:

$$g(y,\,q) = g^0 + q\,g^1 + q^2\,g^2 + \ldots\ldots, \quad (14)$$

where $g(y,\,q)$ may be any of the functions u_s, u_0, T_s, T_0, f_s and f_0. The solution of velocity, temperature and nanoparticle phenomenon (for $q = 1$) are constructed as follows:

$$\begin{aligned} u(y,\,t) = {} & (c_1 + c_7 - 1)\,y + (a_5 + a_{21})\,y^2 + (a_4 + a_{20})\,y^3 \\ & + (a_3 + a_{19})\,y^4 + (a_2 + a_{18})\,y^5 \\ & + (a_1 + a_{17})\,y^6 + a_{16}\,y^7 + a_{15}\,y^8 + a_{14}\,y^9 + a_{13}\,y^{10} \\ & + e^{i\omega t}\left((c_{13} + c_{19} - 1)\,y\right. \\ & + (1 + a_{40} + a_{57})\,y^2 + (a_{39} + a_{56})\,y^3 + (a_{38} + a_{55})\,y^4 \\ & + (a_{37} + a_{54})\,y^5 + (a_{36} + a_{53})\,y^6 + a_{52}\,y^7 + a_{651}\,y^8 \\ & \left. + a_{50}\,y^9 + a_{49}\,y^{10}\right), \end{aligned} \quad (15)$$

$$\begin{aligned} T(y,\,t) = {} & 1 + (c_3 + c_9 - 1)\,y + (a_{10} + a_{30})\,y^2 + (a_9 + a_{29})\,y^3 \\ & + (a_8 + a_{28})\,y^4 + (a_7 + a_{27})\,y^5 \\ & + (a_6 + a_{26})\,y^6 + a_{25}\,y^7 + a_{24}\,y^8 + a_{23}\,y^9 + a_{22}\,y^{10} \\ & + e^{i\omega t}\left((c_{15} + c_{21} - 1)\,y\right. \\ & + (1 + a_{45} + a_{66})\,y^2 + (a_{44} + a_{65})\,y^3 + (a_{43} + a_{64})\,y^4 \\ & + (a_{42} + a_{63})\,y^5 \\ & \left. + (a_{41} + a_{62})\,y^6 + a_{61}\,y^7 + a_{60}\,y^8 + a_{59}\,y^9 + a_{58}\,y^{10}\right), \end{aligned} \quad (16)$$

$$f(y,\,t) = 1 + (c_5 + c_{11} - 1)\,y + (a_{12} + a_{35})\,y^2 + (a_{11} + a_{34})\,y^3$$

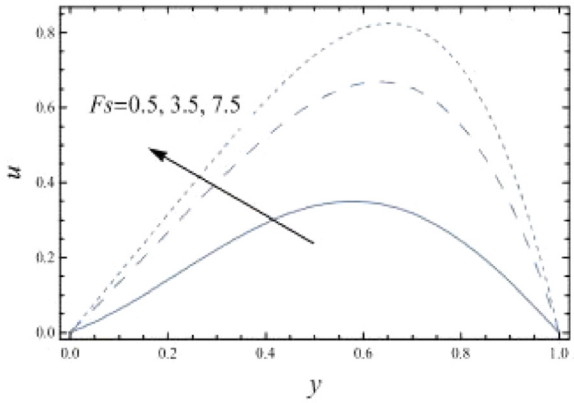

Fig. 2. The velocity profiles are plotted versus y for different values of Fs for a system have the particulars $B_n = 0.05$, Da = 0.1, M = 1, Gr = 1, Br = 1, $Q_1 = 1$, $Q_2 = 1$, Nb = 1.5, Nt = 2.5, Ec = 3, Pr = 0.05, Sc = 1.5, $\delta = 1$; t = 1, and $\omega = 0.5\ \pi$.

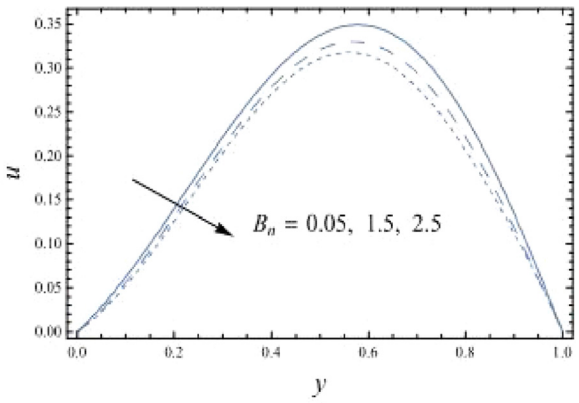

Fig. 3. The velocity profiles are plotted versus y for different values of B_n for a system have the particulars Fs = 0.5, Da = 0.1, M = 1, Gr = 1, Br = 1, $Q_1 = 1$, $Q_2 = 1$, Nb = 1.5, Nt = 2.5, Ec = 3, Pr = 0.05, Sc = 1.5, $\delta = 1$; t = 1, and $\omega = 0.5\ \pi$.

$$
\begin{aligned}
&+a_{33}\,y^4 + a_{32}\,y^5 + a_{31}\,y^6 \\
&+e^{i\omega t}\left((c_{17} + c_{23} - 1)\,y + (1 + a_{48} + a_{71})\,y^2\right. \\
&+(a_{47} + a_{70})\,y^3 \\
&\left.+(a_{46} + a_{69})\,y^4 + a_{68}\,y^5 + a_{67}\,y^6\right), \qquad (17)
\end{aligned}
$$

where a_1 – a_{71} and c_1 – c_{23} are given in the Appendix.

4. Results and discussion

In order to get a physical understanding of the problem and for the purpose of discussing the results, numerical calculations have been performed for the velocity, temperature and nanoparticles phenomena. To discuss the effect of various parameters involved in the problem such as *Fs* B_n, *Ec*, N_t, N_b, Q_1, and Q_2 on the solution of the considered problem, a numerical results are calculated using Mathematica package 7.

Figs. 2 and 3 show the changes of the velocity u versus the normal axis to walls y for different values of Forschheimer number *Fs* and Bingham number B_n. It is seen from these figures that the velocity increases with the increasing values of F_s, whereas it decreases as B_n increases. It is also noted that the velocity for different values of *Fs* and B_n increases with increasing values of normal axis y and reaches a maximum value (at a finite value of y: $y = y_0$) after which it decreases as y increases. The effects of the other parameters are found to be similar to them; these figures are excluded here to avoid any kind of repetition.

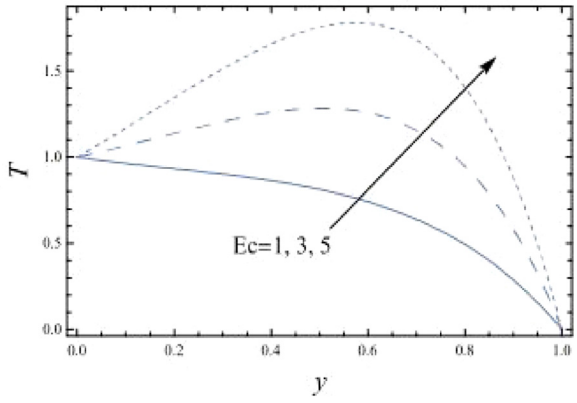

Fig. 4. The temperature profiles are plotted versus y for different values of Ec for a system have the particulars Fs = 0.5, $B_n = 0.05$, Da = 0.1, M = 1, Gr = 1, Br = 1, $Q_1 = 1$, $Q_2 = 1$, Nb = 1.5, Nt = 2.5, Pr = 0.05, Sc = 1.5, $\delta = 1$; t = 1, and $\omega = 0.5\ \pi$.

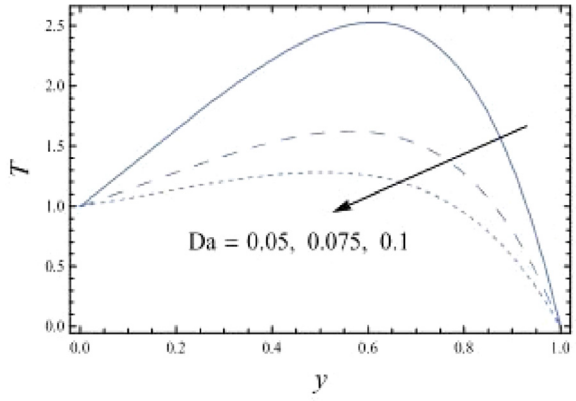

Fig. 5. The temperature profiles are plotted versus y for different values of Da for a system have the particulars Fs = 0.5, $B_n = 0.05$, M = 1, Gr = 1, Br = 1, $Q_1 = 1$, $Q_2 = 1$, Nb = 1.5, Nt = 2.5, Ec = 3, Pr = 0.05, Sc = 1.5, $\delta = 1$; t = 1, and $\omega = 0.5\ \pi$.

Fig. 4 and 5 indicate the variations of the temperature distribution T with the normal axis y for various values of *Ec* and *Da*, respectively. Figs. 4 and 5 indicate that the temperature distribution T increases with increasing the parameter *Ec*, while it decreases by increasing the parameter *Da*, respectively. It is also noted that for large values of *Ec* and small values of *Da*, T is a parabolic function of y, and T increases with y up to a definite value at $y = y_0$ (represents the maximum value of T). For beyond values of y_0, the amount of temperature, T, decreses.. This maximum value of T increases by increasing *Ec*, while it decreases by increasing *Da*. A good agreement with physical expectations is obtained by result in Fig. 4; that there is a rise in the temperature due to the heat created by the viscous dissipation and it is in conformity with the fact that energy is stored in the fluid region due to fractional heating as a consequence of dissipation due to viscosity, and hence the temperature increases as *Ec* increases. The following explains the nonlinear variation of heat transfer. The result in Fig. 4, is in agreement with those obtained by Eldabe and Abouzeid [18].

Heat absorption refers to the heat transfer that occurs between two bodies; it can occur through conduction, convection or radiation. Heat absorption also is an endothermic reaction. The effect of heat absorption parameter q_1 on the temperature distribution T as a function of the dimensionless normal coordinate y is shown in Fig. 6. It is found that the effect of Q_1 on T is found to be exactly similar to the effect of *Da* on T given in Fig. 5 with the only difference that the obtained curves are coincide near the upper wall. Fig. 7 illustrates the effect of the thermophoresis parameter N_t on the temperature distribution T. It is found that the temperature T

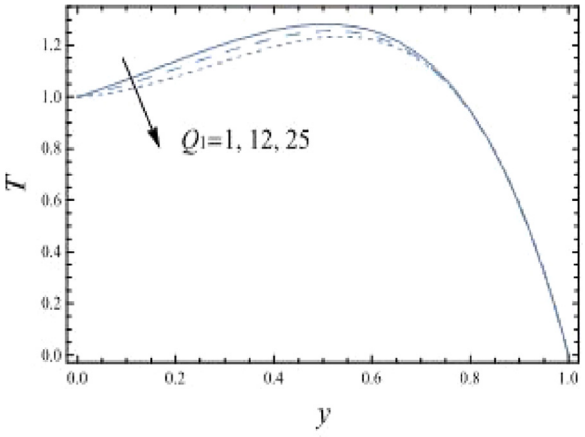

Fig. 6. The temperature profiles are plotted versus y for different values of Q_1 for a system have the particulars Fs = 0.5, B_n = 0.05, Da = 0.1, M = 1, Gr = 1, Br = 1, Q_2 = 1, Nb = 1.5, Nt = 2.5, Ec = 3, Pr = 0.05, Sc = 1.5, δ = 1; t = 1, and $\omega = 0.5\ \pi$.

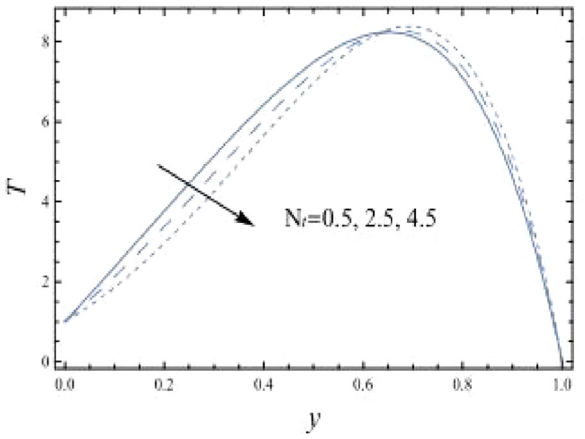

Fig. 7. The temperature profiles are plotted versus y for different values of Nt for a system have the particulars Fs = 0.5, B_n = 0.05, Da = 0.1, M = 1, Gr = 1, Br = 1, Q_1 = 1, Q_2 = 1, Nb = 1.5, Ec = 3, Pr = 0.05, Sc = 1.5, δ = 1; t = 1, and $\omega = 0.5\ \pi$.

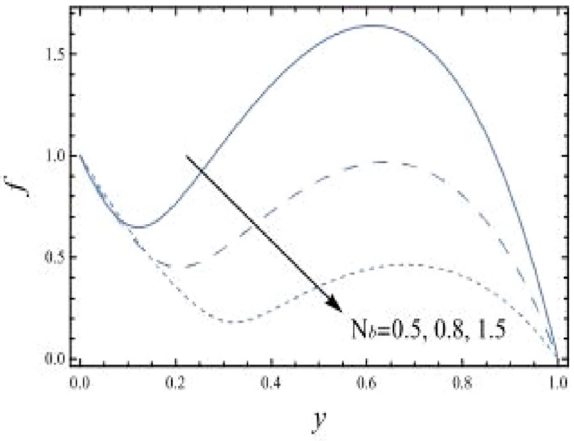

Fig. 8. The nanoparticles profiles are plotted versus y for different values of Nb for a system have the particulars Fs = 0.5, B_n = 0.05, Da = 0.1, M = 1, Gr = 1, Br = 1, Q_1 = 1, Q_2 = 1, Nt = 2.5, Ec = 3, Pr = 0.05, Sc = 1.5, δ = 1; t = 1, and $\omega = 0.5\ \pi$.

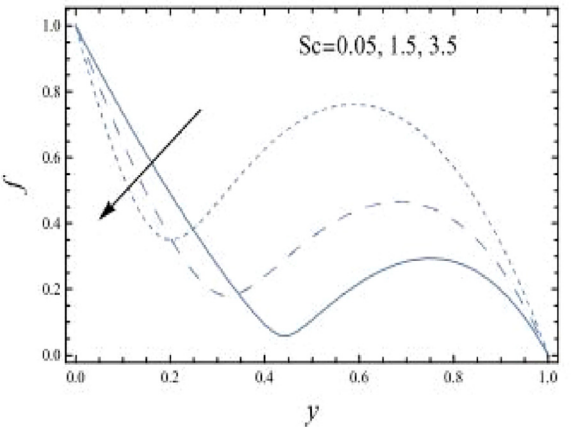

Fig. 9. The nanoparticles profiles are plotted versus y for different values of Sc for a system have the particulars Fs = 0.5, B_n = 0.05, Da = 0.1, M = 1, Gr = 1, Br = 1, Q_1 = 1, Q_2 = 1, Nb = 1.5, Nt = 2.5, Ec = 3, Pr = 0.05, δ = 1; t = 1, and $\omega = 0.5\ \pi$.

increases by increasing N_t in the intervals $y \in [0, 0.65]$; otherwise it decreases by increasing N_t. So, the behavior of T in the interval $y \in [0.65, 1]$, is an inversed manner of its behavior in the other intervals. In this case, for each value of N_t, there are maximum values of T hold at $y = 0.7$. The behavior of T for various values of other parameters is exactly similar to the behavior of T for various values of *Ec* and *Da* given in Figs. 4 and 5.

The nanoparticles phenomena f for different values of Brownian motion parameter N_b is shown in Fig. 8, and it is shown that the nanoparticles phenomena f increases by increasing N_b in the range of y shown in the figure, namely in the interval $y \in [0.1, 1]$, otherwise it decreases as with the increase of N_b near the lower wall. Also for different values of N_b, the nanoparticles phenomena increases with y, till a maximum value (at a finite value of y: $y = y_0$) after which it decreases. Fig. 9 shows that the effect of *Sc* on f is opposite qualitatively behavior for the effect of N_b on f shown in Fig. 8. Figs. 10 and 11 represent the behaviors of the nanoparticles phenomena f with the dimensionless normal coordinate y for different values of heat absorption parameter Q_1 and dimensionless absorption of radiation parameter Q_2, respectively. It is observed from Figs. 10 and 11, that the nanoparticles phenomena f increases with the increase of Q_1, whereas it decreases as Q_2 increases, respectively. It is also noted that the difference of the nanoparticles phenomena f for different values of Q_1 and Q_2 becomes greater with increasing the normal coordinate y and reaches minimum value, after which it increases till a maximum value, then it decreases. The following explains the result in Fig. 11.

The absorption of radiation energy from a higher temperature device to a lower temperature fluid medium. The fluid medium is frequently air, but can also be water, refrigerants or oil. If the fluid medium is water, the heat sink is frequently called a cold plate.

In Figs. 12–14, we make a comparison between our results and those obtained by Eldabe et al. [18]. It is noticed that there is a good agreement.

5. Conclusion

The problem of pulsatile flow with heat transfer of non-Newtonian nanofluid through a non-Darcy porous medium between two permeable parallel vertical plates in the presence of uniform magnetic field is studied. The flow includes free convective, porous medium, viscous dissipation and radiation effects. The main results of our study can be epitomized in the following points:

1) The magnetic field and Brownian motion parameters increase both the flow velocity and temperature but nanoparticles phenomena increases (decreases).
2) The chemical reaction parameter reduces the temperature and hence decreasing the flow velocity, but it increases (decreases) the nanoparticles phenomena.

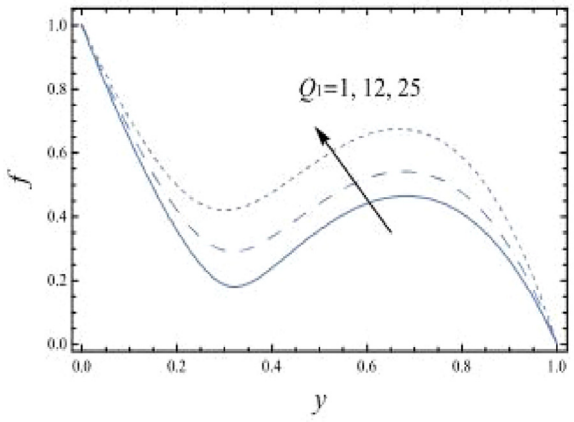

Fig. 10. The nanoparticles profiles are plotted versus y for different values of Q_1 for a system have the particulars Fs = 0.5, B_n = 0.05, Da = 0.1, M = 1, Gr = 1, Br = 1, Q_2 = 1, Nb = 1.5, Nt = 2.5, Ec = 3, Pr = 0.05, Sc = 1.5, δ = 1; t = 1, and $\omega = 0.5\ \pi$.

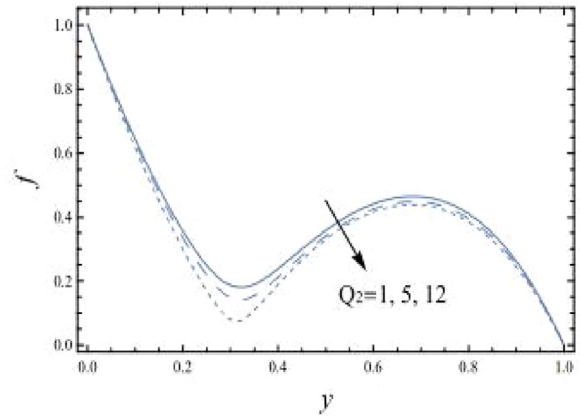

Fig. 11. The nanoparticles profiles are plotted versus y for different values of Q_2 for a system have the particulars Fs = 0.5, B_n = 0.05, Da = 0.1, M = 1, Gr = 1, Br = 1, Q_1 = 1, Nb = 1.5, Nt = 2.5, Ec = 3, Pr = 0.05, Sc = 1.5, δ = 1; t = 1, and $\omega = 0.5\ \pi$.

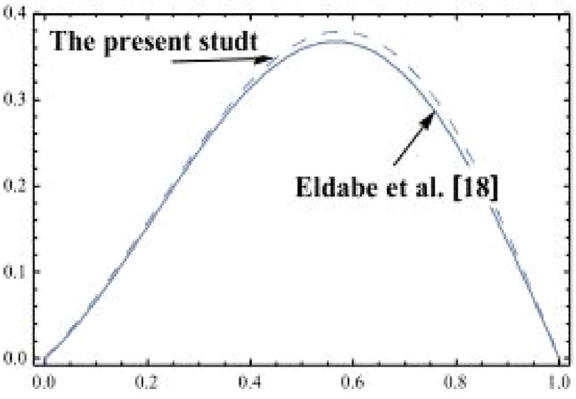

Fig. 12. The velocity profiles are plotted versus y for different values to make a comparison between the present study and Eldabe et al. [18].

3) The flow velocity decreases as the thermophoresis parameter increases, while it decreases (increases) the temperature and nanoparticles phenomena.
4) Both the time and frequency of oscillations decreases the flow velocity, but increases temperature.

Finally, the analytical solutions by using HPM were obtained and the graphical results through Figs. 12–14 showed an excellent agreement with various studies such as Hayat et al. [16] and Eldabe and Abouzeid [24].

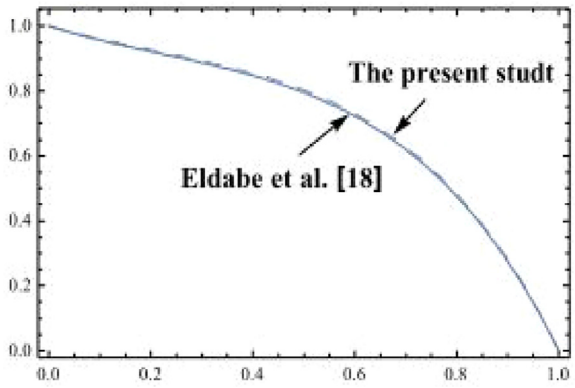

Fig. 13. The temperature profiles are plotted versus y for different values to make a comparison between the present study and Eldabe et al. [18].

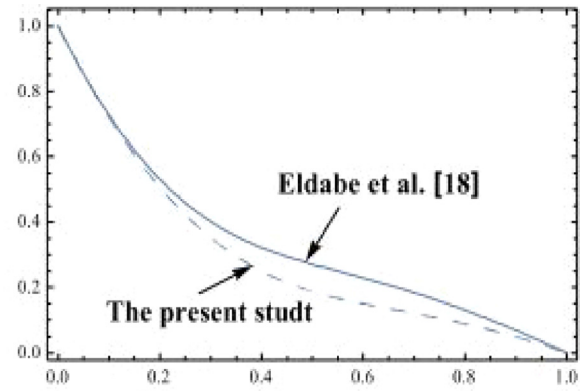

Fig. 14. The nanoparticles profiles are plotted versus y for different values to make a comparison between the present study and Eldabe et al. [18].

Acknowledgment

We'd like to thank the reviewers for review and highly appreciate the comments and suggestions, which significantly contributed to improve the quality of the modified paper.

Appendix

In order to save space, the mathematical formulas of the constants a_1 – a_{71} and c_1 – c_{23} are not included here. However, they are available upon request from the author.

References

[1] N. Anbuchezhian, K. Srinivasan, K. Chandrasekaran, R. Kandasamy, Thermophoresis and Brownian motion effects on boundary layer flow of nanofluid in presence of thermal stratification due to solar energy, Appl. Math. Mech. 33(2012) 765–780.
[2] T. Hayat, S. Qayyum, M. Imtiaz, A. Alsaedi, Comparative study of silver and copper water nanofluids with mixed convection and nonlinear thermal radiation, Int. J. Heat. Mass Transfer 102 (2016) 723–732.
[3] T. Hayat, S. Qayyum, A. Alsaedi, A. Shafiq, Inclined magnetic field and heat source/sink aspects in flow of nanofluid with nonlinear thermal radiation, Int. J. Heat. Mass Transfer 103 (2016) 99–107.
[4] U. Akdag, S. Akcay, D. Demiral, Heat transfer enhancement with laminar pulsating nanofluid flow in a wavy channel, Int. Comm. Heat Mass Transfer 59 (2014) 17–23.
[5] T. Hayat, A. Shafiq, M. Imtiaz, A. Alsaedi, Impact of melting phenomenon in the Falkner–Skan wedge flow of second grade nanofluid: a revised model, J. Mol. Liq. 215 (2016) 664–670.
[6] T. Hussain, S. Hussain, T. Hayat, Impact of double stratification and magnetic field in mixed convective radiative flow of Maxwell nanofluid, J. Mol. Liq. 220 (2016) 870–878.

[7] F. Selimefendigil, H.F. Öztop, Identification of forced convection in pulsating flow at a backward facing step with a stationary cylinder subjected to nanofluid, Int. Comm. Heat Mass Transfer 45 (2013) 111–121.
[8] T. Hayat, M. Imtiaz, A. Alsaedi, Melting heat transfer in the MHD flow of Cu–water nanofluid with viscous dissipation and Joule heating, Adv. Power Tech. 27 (2016) 1301–1308.
[9] T. Hayat, A. Aziz, T. Mohamed, B. Ahmed, On magnetohydrodynamic flow of second grade nanofluid over a nonlinear stretching sheet, J. Magn Magn Mater. 27 (2016) 1301–1308.
[10] M. Rahgoshay, A.A. Ranjbar, A. Ramiar, Laminar pulsating flow of nanofluids in a circular tube with isothermal wall, Int. Comm. Heat Mass Transfer 39 (2012) 463–469.
[11] P. Forchheimer, Wasserbewegung durch boden, Forschtlft Ver. D. Ing. 45 (1901) 1782–1788.
[12] S. Shehjzad, F. Abbasi, T. Hayat, A. Alsaedi, Cattaneo-Christov heat flux model for Darcy-Forchheimer flow of an Oldroyd-B fluid with variable conductivity and non-linear convection, J. Mol. Liq. 224 (2016) 274–278.
[13] T. Hayat, T. Mohamed, S. Almezal, S. Liao, Darcy-Forchheimer flow with variable thermal conductivity and Cattaneo-Christov heat flux, Int. J. Numer. Method Heat Fluid Flow 26 (2016) 2355–2369.
[14] N.T. Eldabe, S.M. Elmohandis, Pulsatile magnetohydrodynamic viscoelastic flow through a channel bounded by two permeable parallel plates, J. Phys. Soc. Jpn. 64 (11) (1995) 4163–4174.
[15] N.T. Eldabe, S.M. Elmohandis, Effect of couple stresses on pulsatile poiseuille flow", Fluid Dyn. Res. 15 (1995) 313–324.
[16] T. Hayat, A. Tanveer, F. Abbasi, G. Mousa, Impact of radial magnetic field on peristalsis in curved channel with convective boundary conditions, J. Magn Magn Mater. 403 (2016) 47–59.
[17] P. Chaturani, P.K. Nandal, Mathematical model of pulsatile flow of blood, Int. J. Eng. Sci 38 (2000) 215–238.
[18] N.T. Eldabe, M.A. Hassan, W.A. Godh, Unsteady magnetohydrodynamic free convection flow past a semi-infinite permeable moving plate through porous medium with chemical reaction and radiation absorption, J. Heat Transfer 135 (2013) 1–5 024501.
[19] M.F. El-Sayed, N.M.T. Eldabe, A.Y. Ghaly, H.M. Sayed, Magnetothermodynamic peristaltic flow of Bingham non-Newtonian fluid in eccentric annuli with slip velocity and temperature jump conditions, J. Mech. 29 (2013) 493–506.
[20] J.H. He, Homotopy perturbation technique, Comput. Methods Appl. Mech. Eng. 178 (1999) 257–262.
[21] M.Y. Abou-zeid, Homotopy perturbation method to gliding motion of bacteria on a layer of power-law nanoslime with heat transfer, J. Comput. Theor. Nanosci. 12 (2015) 3605–3614.
[22] M.Y. Abou-zeid, Homotopy perturbation method to MHD non-Newtonian nanofluid flow through a porous medium in eccentric annuli with peristalsis, Thermal Sci. (2015), doi:10.2298/TSCI150215079A.
[23] M.Y. Abou-zeid, Effects of thermal-diffusion and viscous dissipation on peristaltic flow of micropolar non-Newtonian nanofluid: Application of homotopy perturbation method, Results Phys 6 (2016) 481–495.
[24] N.T. Eldabe, M.Y. Abou-zeid, Magnetohydrodynamic peristaltic flow with heat and mass transfer of micropolar biviscosity fluid through a porous medium between two co-axial tubes, Arab J. Sci. Eng. 39 (2014) 5045–5062.